

Polarization-sensitive ultraviolet photodetectors based on *M*-plane GaN grown on LiAlO₂ substrates

C. Rivera,^{a)} J. L. Pau, and E. Muñoz

ISOM and Departamento Ingeniería Electrónica, ETSI Telecomunicación, Universidad Politécnica de Madrid, Ciudad Universitaria, 28040 Madrid, Spain

P. Misra, O. Brandt, H. T. Grahn, and K. H. Ploog

Paul-Drude-Institut für Festkörperelektronik, Hausvogteiplatz 5-7, 10117 Berlin, Germany

(Received 29 December 2005; accepted 5 April 2006; published online 25 May 2006)

Polarization-sensitive photodetectors for the ultraviolet spectral range based on *M*-plane GaN films grown on LiAlO₂ substrates have been fabricated and characterized. These detectors exploit the dichroic properties of strained, *M*-plane GaN films. For a 400-nm-thick film, a maximum contrast of 7.25 between the detection of light polarized perpendicular and parallel to the *c*-axis is reached at 363 nm. Considerations for the detector design show that thin strained *M*-plane GaN films will enhance the polarization-sensitive bandwidth, while the maximum contrast can be obtained for relaxed thick films under weak signal detection conditions. © 2006 American Institute of Physics. [DOI: 10.1063/1.2206128]

Light polarization control is of great importance in a wide range of scientific and technological areas. For semiconductor optoelectronic devices, polarization control is usually obtained as a consequence of the selection rules in low-dimensional structures fabricated along low-symmetry directions. The realization of polarized light-emitting diodes,¹ tunable polarization converters,² polarization threshold switches,³ and polarization-sensitive photodetectors^{4,5} (PSPDs) has been reported. One mechanism to increase the optical anisotropy and therefore the polarization sensitivity is the application of anisotropic strain, which reduces the symmetry of the crystal structure. Currently, there is an increasing interest in the control of the polarization state for the ultraviolet (UV) spectral range, in particular, for data storage, sensing applications, and biophotonics. UV PSPDs based on *M*-plane GaN were proposed a few years ago by Ghosh *et al.*⁶ *M*-plane group-III nitrides exhibit highly anisotropic optical properties that allow for the polarization-sensitive detection in the visible and UV spectral ranges. The anisotropy can be further enhanced by the presence of in-plane anisotropic strain generated by the lattice mismatch between GaN and the LiAlO₂ substrate. Both static⁷ and dynamic⁸ polarization rotations have been recently demonstrated, achieving polarization rotation angles as high as 40° (static) and 35° (dynamic). Theoretical studies and photoreflectance (PR) spectra have revealed that the anisotropic strain generated in *M*-plane films grown on LiAlO₂ substrates leads to modifications of the valence band structure (VBS) so that the two interband transitions in the vicinity of the energy gap become completely linearly polarized either parallel ($E \parallel c$) or perpendicular to the *c* axis ($E \perp c$).⁹

In this letter, we describe the fabrication and performance of PSPDs based on anisotropically strained *M*-plane GaN films on LiAlO₂. In addition, we discuss some important issues for the design of such photodetectors.

The *M*-plane GaN film was grown by rf plasma-assisted molecular-beam epitaxy (PAMBE) on a γ -LiAlO₂(100) substrate.¹⁰ The *M*-plane orientation of the film and its single

phase nature (i.e., lack of *C*-plane-oriented inclusions) were verified by means of triple-axis high-resolution x-ray diffraction (HRXRD). The HRXRD also showed that the *M* plane was under biaxial compressive strain with an out-of-plane tensile strain of $\epsilon_{yy}=0.43\%$ (cf. inset of Fig. 1 for the choice of coordinates in the wurtzite unit cell of GaN). A film thickness of 400 nm was determined by scanning electron microscopy. The carrier concentration in the sample studied was about $3.5 \times 10^{15} \text{ cm}^{-3}$ (*n* type) as extracted from capacitance-voltage (*C-V*) measurements of metal-insulator-semiconductor (MIS) diodes, indicating a complete depletion of the *M*-plane GaN film.

Both semitransparent Schottky barrier and MIS structures were fabricated on *M*-plane GaN films as PSPDs. We used a planar geometry to form the contacts. The semitransparent electrode was made of Au (12 nm), while the pad contacts were made of Ni (50 nm)/Au (200 nm) and Ti (50 nm)/Al (200 nm) for the rectifying and Ohmic electrodes, respectively. The insulator used in the MIS structures was a 120-nm-thick SiN_x layer deposited by plasma-enhanced chemical vapor deposition.

Photoluminescence (PL), photocurrent, and *C-V* measurements were performed on these PSPDs. Continuous-wave (cw) PL was excited with the 244 nm line from a second harmonic generator pumped by an Ar⁺ laser. Photocurrent spectra for front illumination were obtained in the 325–400 nm range by using a linearly polarized beam from a 150 W xenon arc lamp filtered by a monochromator. The dependence of the photocurrent on the in-plane polarization angle φ of the incident beam, where $\varphi=0^\circ$ corresponds to $E \parallel c$, was carried out by rotating the sample keeping the polarization of the incident beam fixed. The relative responsivity was then determined by normalizing the photocurrent to the system's response measured with a calibrated Si photodiode. The absolute responsivity was accurately determined using a He–Cd laser (325 nm). The *C-V* characteristics were measured using an HP4284A impedance analyzer with 50 mV test signal at 10 kHz.

The effect of the in-plane anisotropic strain in the *M*-plane GaN film on the optical polarization properties has

^{a)}Electronic mail: crivera@die.upm.es

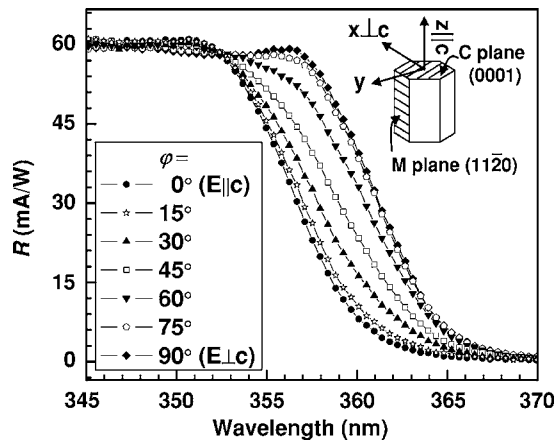


FIG. 1. Photocurrent spectra for different in-plane polarization angles φ under normal incidence at room temperature. Inset: The unit cell of the wurtzite crystal structure of GaN and the choice of coordinates.

been mainly studied by polarized PR spectroscopy.⁹ As mentioned above, the strain dependence of the calculated oscillator strengths shows that the transitions E_1 , E_2 , and E_3 between the three uppermost valence bands and the conduction band are predominantly x , z , and y polarized, respectively.⁹ In this work, given the out-of-plane strain (ϵ_{yy}) obtained by HRXRD, we extracted the in-plane components for the perpendicular (ϵ_{xx}) and parallel (ϵ_{zz}) strain components with respect to the c axis from cw PL at 10 K using the VBS parameters of Ref. 11, resulting in $\epsilon_{xx} = -0.93\%$ and $\epsilon_{zz} = -0.30\%$ (the negative values indicate compressive strain). For this determination, PL transitions at 3.505 and 3.561 eV corresponding to the E_1 and E_2 transitions were studied as a function of the polarization state of the incident beam. Details about this study will be published elsewhere.

The measured photoresponse changes linearly as a function of excitation power in the measured range from 2×10^{-5} to 1 W/cm^2 . Its dependence on the in-plane polarization angles φ is shown in Fig. 1 for the Schottky barrier photodiodes in the photovoltaic mode. Figure 1 clearly shows that the photodetection edge is blueshifted as the polarization of the incoming light changes from $\mathbf{E} \perp \mathbf{c}$ to $\mathbf{E} \parallel \mathbf{c}$. The peak value of the responsivity R for $\mathbf{E} \perp \mathbf{c}$ is as high as 60 mA/W , being slightly higher for $\mathbf{E} \parallel \mathbf{c}$. Calculations using the VBS parameters of Ref. 11 support this result, since the joint density of states is also slightly higher (about 5%) for the E_1 state than for the E_2 state. We found modulation features in the photocurrent spectra, which can be associated with band mixing effects at higher energies (e.g., between the E_1 and E_2 states). In the case of $\mathbf{E} \perp \mathbf{c}$, the photocurrent has a relative minimum at 353 nm, whereas for $\mathbf{E} \parallel \mathbf{c}$ a similar modulation is observed at 347 nm.

In order to determine the polarization sensitivity near the band gap, we measured the spectral dependence of the contrast for $\mathbf{E} \perp \mathbf{c}$ and $\mathbf{E} \parallel \mathbf{c}$ as shown in Fig. 2. A maximum contrast $R_{\perp}/R_{\parallel} = 7.25$ is reached at 363 nm, where R_{\perp} and R_{\parallel} are the components of the responsivity for $\mathbf{E} \perp \mathbf{c}$ and $\mathbf{E} \parallel \mathbf{c}$, respectively. Note that the maximum contrast occurs below the maximum of R_{\perp} , but in a wavelength range where R_{\parallel} is already rather small. This maximum value of the contrast is limited by the absorption below the GaN band gap (the theoretical oscillator strength ratio for $\mathbf{E} \perp \mathbf{c}$ and $\mathbf{E} \parallel \mathbf{c}$ is larger in this region). The origin of the absorption below the energy gap can be extrinsic or defect related as frequently observed

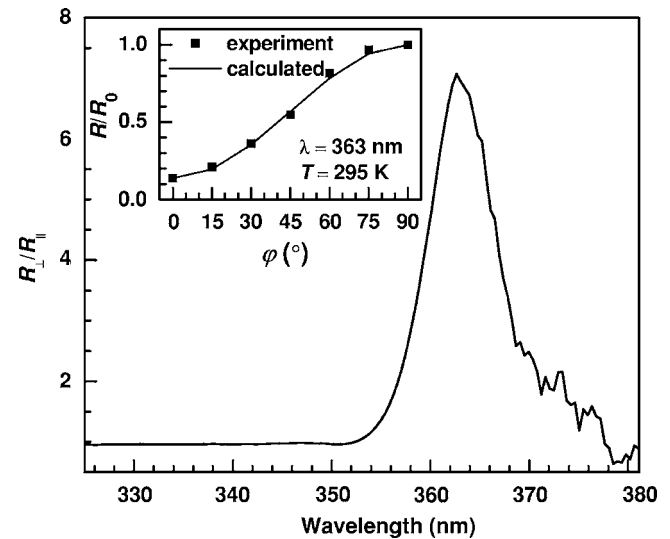


FIG. 2. Contrast of the responsivities for polarization perpendicular (R_{\perp}) and parallel (R_{\parallel}) to the c axis at room temperature. Inset: Responsivity R as a function of the in-plane polarization angle φ (squares) and fit (lines) using Eq. (1).

in GaN.¹² Note that, while the dislocation density in M -plane GaN grown on LiAlO_2 is much lower than in conventional C -plane GaN films, the density of stacking faults (SFs) is much higher for M -plane GaN.^{13,14} However, SFs will mainly affect the electrical properties. The polarization-sensitive bandwidth is defined at the half-maximum responsivity, resulting for Schottky photodetectors in a room-temperature value of $7.7 \pm 0.4 \text{ nm}$ (72.6 meV) at 363 nm. This bandwidth cannot be directly compared with the energy splitting between the E_1 and E_2 states, since other extrinsic factors such as the absorption below the band gap and the layer thickness must be taken into account for the PSPD photoresponse. However, since the photoresponse is proportional to the incident power, we can express the angular dependence of the in-plane polarization of the responsivity as follows:

$$R = R_{\perp} \sin^2(\varphi) + R_{\parallel} \cos^2(\varphi). \quad (1)$$

The inset in Fig. 2 shows that the experimental result can be well described by Eq. (1) at the peak wavelength of the contrast. Consequently, we can characterize the full photoresponse for an arbitrary polarization angle φ by its R_{\perp} and R_{\parallel} components.

The thickness of the M -plane GaN film plays an important role in the design of PSPDs. Both the actual in-plane strain values and the total absorption of the film depend on its thickness. On one hand, the in-plane strain values determine the valence band splitting and, therefore, are related to the polarization-sensitive bandwidth. As thicker films gradually relax, their valence band splitting becomes more and more comparable to the value of a typical unstrained GaN film. On the other hand, the optimum film thickness t^* for a photodetector to obtain the maximum R_{\perp}/R_{\parallel} contrast also takes into account other device parameters according to

$$t^* \approx \frac{1}{\alpha_{\perp} - \alpha_{\parallel}} \ln \left\{ \frac{i_0 (1 - r_{\perp}) \alpha_{\perp}}{[K(1 - r_{\perp}) + i_0] (1 - r_{\parallel}) \alpha_{\parallel}} \right\}, \quad (2)$$

where t^* is calculated by maximizing the ratio between the photocurrents $I_{\text{ph},j} = K(1 - r_j)[1 - \exp(-\alpha_j t^*)] + i_0$ detected for perpendicular ($j = \perp$) and parallel ($j = \parallel$) polarizations. In Eq.

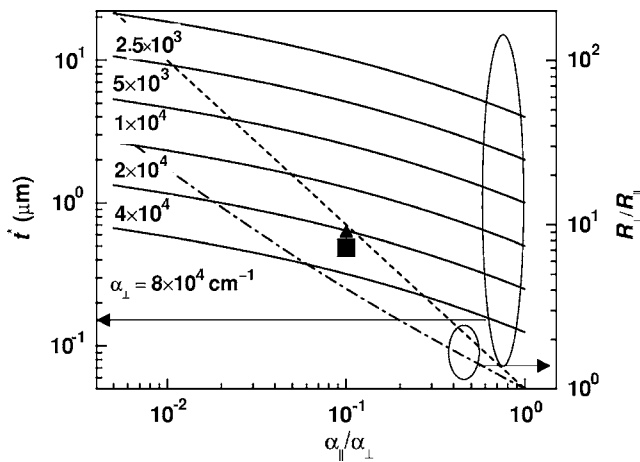


FIG. 3. Optimum photodetector film thickness t^* as a function of $\alpha_{\parallel}/\alpha_{\perp}$ for different values of α_{\perp} calculated using Eq. (2). The maximum contrast R_{\perp}/R_{\parallel} calculated for the t^* values of the two different optimization limits when $i_0 \ll K(1-r_{\perp})$ (dotted line) and $i_0 \gg K(1-r_{\perp})$ (dash-dotted line) is also shown. The square corresponds to the experimental result for the investigated sample with a thickness of 400 nm. The vertical arrow shows that the contrast R_{\perp}/R_{\parallel} measured in our sample is close to its maximum value.

(2), K and i_0 are constants related to I_{ph} and α_{\perp} (α_{\parallel}) and r_{\perp} (r_{\parallel}) are the absorption and reflection coefficients for $\mathbf{E} \perp \mathbf{c}$ ($\mathbf{E} \parallel \mathbf{c}$), respectively. More specifically, i_0 is the dark current contribution to the detected signal (i.e., current noise), which will become more important as the incident power becomes weaker. In the derivation of Eq. (2), we have assumed that $\alpha_{\parallel} \ll \alpha_{\perp}$, since in the dichroic regime α_{\parallel} is usually more than one order of magnitude smaller than α_{\perp} . The same solution as Eq. (2) is obtained by maximizing R_{\perp}/R_{\parallel} , where $R_j = I_{\text{ph},j}/P$ with P denoting a constant for maximization purposes. In general, the film thickness will be optimized for detection at the R_{\perp}/R_{\parallel} contrast peak (e.g., 363 nm in Fig. 2). We can derive two different limits for Eq. (2), depending on the weight of i_0 in the device photocurrent. In the first case, when i_0 is negligible compared to $K(1-r_{\perp})$ (i.e., high power regime), t^* will eventually reach negative values, in particular, for $\alpha_{\parallel}/\alpha_{\perp}$ ratios closer to unity. Since only positive values are physically attainable, we will consider that t^* tends to zero. In this case, the maximum achievable sensitivity $(R_{\perp}/R_{\parallel})_{\text{max}}$ or its asymptotic behavior is given by

$$\left(\frac{R_{\perp}}{R_{\parallel}}\right)_{\text{max}} = \frac{(1-r_{\perp})\alpha_{\perp}}{(1-r_{\parallel})\alpha_{\parallel}}. \quad (3)$$

In the second case, under weak signal detection, when i_0 becomes comparable to the photocurrent, t^* will be better optimized for thicker layers. However, the approximation $\alpha_{\parallel} \ll \alpha_{\perp}$ is not necessary for $i_0 \gg K(1-r_{\perp})$ (weak signal detection limit). Note that Eq. (2) approaches the exact solution of the $R_{\perp}-R_{\parallel}$ maximization problem as $K(1-r_{\perp})$ becomes negligible in comparison with i_0 . Therefore, we will consider the weak signal detection optimization as a maximization problem of $R_{\perp}-R_{\parallel}$ instead of R_{\perp}/R_{\parallel} .

Figure 3 shows a contour plot of t^* as a function of $\alpha_{\parallel}/\alpha_{\perp}$ for different values of α_{\perp} under weak signal conditions (the second case). From Fig. 3, it is clear that t^* increases as $\alpha_{\parallel}/\alpha_{\perp}$ decreases. For values of $\alpha_{\parallel}/\alpha_{\perp}$ closer to unity, t^* is obtained for rather thin films, which maximize

both bandwidth and R_{\perp}/R_{\parallel} contrast. The same behavior is found for the first case [$i_0 \ll K(1-r_{\perp})$], but the t^* curves are shifted to lower values. In the general case, t^* will lie between zero and the values shown in Fig. 3 depending on the weight of i_0 in the detected photocurrent. At the same time, the R_{\perp}/R_{\parallel} contrast will be optimized between the values given by Eq. (3) marked by the dotted line and the R_{\perp}/R_{\parallel} values for t^* obtained under weak signal conditions marked by the dash-dotted line shown in Fig. 3. Note that, while the device can operate in different signal-to-noise ratio conditions, the R_{\perp}/R_{\parallel} values are always determined by ignoring the i_0 term. We suggest to design devices with film thicknesses close to t^* optimized under weak signal detection conditions to maintain a minimum quantum efficiency. Furthermore, this thickness maximizes $R_{\perp}-R_{\parallel}$ regardless of the i_0 values.

In summary, we have demonstrated the operation of M -plane GaN-based dichroic photodetectors, where the intrinsic optical anisotropy is enhanced by the anisotropic strain generated by the mismatch between the GaN film and the LiAlO₂ substrate. The responsivity of the PSPDs can be expressed using two orthogonal polarization components, which are perpendicular and parallel to the c axis. The performance of the photodetector depends critically on the film thickness. While thicker films are suitable for highly selective M -plane GaN epilayers, i.e., small values of $\alpha_{\parallel}/\alpha_{\perp}$, thinner films are preferred for values of $\alpha_{\parallel}/\alpha_{\perp}$ closer to unity. In order to optimize the photodetector performance, these results have to be taken into account in the device design together with the dependence of the in-plane strain on the film thickness.

The authors would like to acknowledge J. M. Calleja for kindly providing the polarizer system. Partial financial support from projects EU STREP 505641-1, MEC MAT2004-02875, and CAM GR/MAT/0042/2004 is acknowledged.

¹N. F. Gardner, J. C. Kim, J. J. Wierer, Y. C. Shen, and M. R. Krames, Appl. Phys. Lett. **86**, 111101 (2005).

²R. Wirth, A. Moritz, C. Geng, F. Scholz, and A. Hangleiter, Appl. Phys. Lett. **69**, 2225 (1996).

³E. Greger, P. Riel, M. Moser, T. Kippenberg, P. Kiesel, and G. H. Döhler, Appl. Phys. Lett. **71**, 3245 (1997).

⁴H. Temkin, M. B. Panish, and R. A. Logan, Appl. Phys. Lett. **47**, 978 (1985).

⁵J. Wang, M. S. Gudixsen, X. Duan, Y. Cui, and C. M. Lieber, Science **293**, 1455 (2001).

⁶S. Ghosh, O. Brandt, H. T. Grahn, and K. H. Ploog, Appl. Phys. Lett. **81**, 3380 (2002).

⁷P. Misra, Y. J. Sun, O. Brandt, and H. T. Grahn, J. Appl. Phys. **96**, 7029 (2004).

⁸K. Omae, T. Flissikowski, P. Misra, O. Brandt, H. T. Grahn, K. Kojima, and Y. Kawakami, Appl. Phys. Lett. **86**, 191909 (2005).

⁹S. Ghosh, P. Waltereit, O. Brandt, H. T. Grahn, and K. H. Ploog, Phys. Rev. B **65**, 075202 (2002).

¹⁰P. Waltereit, O. Brandt, M. Ramsteiner, R. Uecker, P. Reiche, and K. H. Ploog, J. Cryst. Growth **218**, 143 (2000).

¹¹U. Behn, P. Misra, H. T. Grahn, B. Imer, S. Nakamura, S. P. DenBaars, and J. S. Speck, Appl. Phys. Lett. **88**, 161920 (2006).

¹²M. A. Reshchikov and H. Morkoç, J. Appl. Phys. **97**, 061301 (2005).

¹³Y. J. Sun, O. Brandt, U. Jahn, T. Y. Liu, A. Trampert, S. Cronenberg, S. Dhar, and K. H. Ploog, J. Appl. Phys. **92**, 5714 (2002).

¹⁴T. Y. Liu, A. Trampert, Y. J. Sun, O. Brandt, and K. H. Ploog, Philos. Mag. Lett. **84**, 435 (2004).